

Review of Bearingless Motor Technology for Significant Power Applications

Jiahao Chen, Jingwei Zhu, Eric L Severson

Department of Electrical and Computer Engineering

University of Wisconsin-Madison

Madison, Wisconsin 53706

Email: eric.severson@wisc.edu

Abstract—This paper reviews bearingless motor technology for medium and high power applications. Historically, bearingless motors have resided in research settings and certain niche commercial applications. Significant literature has been dedicated to developing designs that feature highly-specific geometry, restricted by applications with a unique set of needs, oftentimes with low power requirements. The first part of this paper reviews existing and potentially new use-cases of magnetic levitation in transportation and industrial applications. The second part of the paper reviews bearingless motor technology for these applications, presents a comprehensive literature review of prototype test results, and highlights efforts to generalize and increase the power rating of bearingless motor technology. The final part of this paper derives sizing equations of different bearingless motor topologies, which are summarized as a design tool for developing industrial-scale bearingless motor technology.

Index Terms—bearingless motor, high speed motor, combined winding, magnetic bearings, self-bearing motor.

I. INTRODUCTION

Contact-type bearings are typically the first components to fail in an electric motor system. The recent introduction of commercial wide-bandgap semiconductor switching devices allows motor drives to efficiently operate at higher fundamental frequencies, enabling motor designs to feature a higher number of poles as well as higher rotational speeds. Both of these design aspects enable higher power density motor designs, and have been instrumental in developing new transportation electrification concepts [1], [2], especially given the ability of high speed motors to match the rotational speed of the load and eliminate any need for a gearbox. However, increasing rotational speeds shortens the bearing lifetime—a critical concern for transportation and industrial applications. Additionally, bearing lubricants can interfere with the broader system a motor is used in. Finally, bearings are a source of frictional losses in motor systems. While these losses are often insignificant for low bearing DN values (diameter \times r/min), they can become significant at high peripheral speeds or in extreme thermal environments.

For these reasons, non-contact bearing systems have received recent commercial attention for motor systems. There are three primary technology divisions for non-contact bearings: oil lubricated journal bearings, passive air-foil bearings and magnetic suspension. The first, oil lubricated journal bearings, have high load-carrying capacity [3], and are commonplace in large machinery, but have stability challenges at high

rotational speeds [4]. The second, air-foil bearings, provide a purely passive, mechanical solution that has been successful for smaller shafts, over a specific speed range, and in non-vacuum environments [5], [6]. Commercial applications include super chargers, industrial blowers and aeration equipment, and gas micro-turbine generators [5], [7]–[10].

The third approach, magnetic levitation, has been commercialized in the form of active magnetic bearings (AMBs). This technology can work for nearly any size shaft, any speed range, and any operating condition. The active control of the magnetic suspension can be used to modify rotor dynamics in real time, i.e. to avoid critical speeds. There are several commercial AMB products that existing motor systems can be retrofitted to use. This technology has been deployed in many different applications over various speed and power levels, described in Section II.

The low force density of magnetic bearings causes two key problems: first, it reduces the power density of the overall motor system, which is particularly problematic for designers looking for non-contact bearings to enable high rotational speeds as a means of increasing power density. Second, magnetic bearings occupy a significant portion of the shaft's axial length, meaning that the shaft space cannot be used by the motor. The maximum length of a motor system shaft is typically limited to avoid flexible modes. For a given maximum rotational speed, this means that the length of the magnetic bearing reduces the designable power rating of the motor system, an effect that becomes especially problematic as speeds exceed 100,000 r/min. Finally, AMBs are expensive and complicated to integrate. Bearingless motors have the potential to solve the shortcomings of AMBs by integrating the functionality of one or more AMBs into an electric motor.

This paper considers the design of magnetic suspension systems based around bearingless motor technology for direct drive applications in transportation electrification and industrial compressors. The paper first reviews current and potential use-cases for AMBs and bearingless motors. The paper then reviews bearingless motor technology and highlights development efforts to generalize this technology for large transportation and industrial applications. Finally, the paper presents a sizing analysis illustrating how torque and suspension force ratings scale with bearingless machine size.

A conference version of this paper was published previously as [11]. Since then, the authors have added a comprehensive

literature review and analysis of experimental test results of bearingless motors as well as a comparative optimization of techniques to maximize design performance for medium and high power levels.

II. APPLICATIONS FOR MAGNETIC LEVITATION

This section reviews current and potential use-cases for magnetic levitation in transportation and industrial applications. Bearingless motors have the potential to solve several shortcomings of AMBs; however, current bearingless technology cannot yet meet the power requirements of these application spaces (which are highlighted in this section). The highest power published bearingless motor experimental results are at approximately 30 kW [12], [13]. The only successful commercial deployment of bearingless motors has been for low power applications. Examples include ventricle assist devices [14], hygienic pumps and mixing devices [15], and Lorentz-type bearingless motors for optical systems [16].

A. Transportation Electrification

Magnetic levitation is increasingly being considered for use in transportation subsystems as a means of enabling higher efficiency (range increases), higher rotational speeds (size reduction), and intelligent self-monitoring. Three application areas are identified in this paper: waste heat recovery for vehicle electric loads, aircraft engines and starter/generators, and electric assist turbochargers (e-turbochargers). An additional area is described, which is not completely levitated: in-wheel landing gear motors for aircraft taxiing.

Organic Rankine Cycle (ORC) systems enable low temperature waste heat recovery. This technology has been commercialized for stationary applications and is gaining attention for mobile applications, such as ships, rail, and city buses [17]. Magnetic bearings are currently used to facilitate efficient operation of compact, high speed generators [18]. This has recently been commercialized for marine applications in the form of an engine water jacket with a 125 kW permanent magnet motor supported by AMBs [19].

The potential use of AMBs in aircraft engines and starter/generators is discussed in [20], [21] to enable completely oil-free, low maintenance systems. Several patent applications have been filed on these concepts, for example: [22], [23]. One of the key challenges in this space is reliable AMB operation at high temperatures.

Turbocharger, e-turbocharger, and supercharger technology has been developed for automobiles as a means of increasing efficiency and performance. These systems typically have high rotational speeds (50,000–300,000 r/min), to minimize their size and weight, and operate under high temperature conditions, all of which places strain on their bearing systems [24]–[27]. It is estimated that 80% of turbocharger failures are due to bearing problems from hydrodynamic or contact bearings [27]. Several patent applications have been filed around magnetically levitated turbochargers with both passive and active magnetic bearings as well as a bearingless motor concepts, for example [27]–[31]. E-turbocharger motor/generator power ratings vary from 1 to > 100 kW. The bulky nature of AMBs

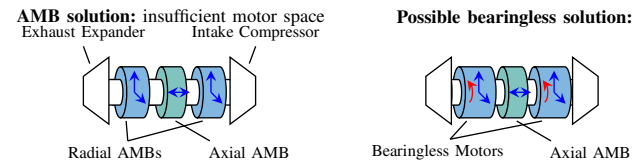


Fig. 1. Magnetically levitated e-turbocharger concept.

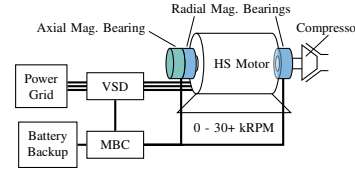


Fig. 2. Industrial compressor system with magnetic bearings. VSD: Variable Speed Drive; MBC: Magnetic Bearing Controller; HS: High Speed.

has prevented their use in the highest speed e-turbocharger designs because there is insufficient shaft space available for both the AMB system and the motor/generator, depicted in Fig. 1. Superchargers differ from turbochargers and e-turbochargers in that they eliminate the exhaust expansion stage and instead rely completely on the electric motor for powering the air intake [32]. This technology may be especially suitable for a bearingless motor because the lower operating temperatures are more compatible with permanent magnet rotors.

In addition to these fully levitated applications, conical, bearingless motors capable of controlled axial movement are under development as in-wheel motors in aircraft landing gear [33], [34]. The rotor is supported radially via bearings, but can be controlled to travel in the axial direction to disengage from the stator during take-off and landing (when the high rotational speeds may cause problematic back-EMF levels) and to re-engage when on the runway to taxi the aircraft.

B. Industrial Applications

Several papers have reported on the suitability of magnetic bearings for use in industry, which are now highlighted. A typical topology for a magnetic bearing equipped large fluid-handling industrial motor system is shown in Fig. 2.

In [35], Knopse reviews research on developing AMBs to overcome lifetime and damping limitations in rolling element bearings for high speed machine tools. Experimental results are presented for a 30,000 r/min, 67 kW induction motor with AMBs. One of the primary limitations noted is that AMBs' inherently low specific load capacity yields elongated designs, which can cause rotor dynamic challenges.

In [36], Kasarda presents the history of magnetic levitation and highlights several industrial deployments of active magnetic bearings in the 1990s. These deployments include turbomachinery, primarily in large compressors for natural gas transportation where motor power requirements ranged from a few kilowatts up to 29 MW and with maximum rotational speeds of 60,000 r/min. Other applications reviewed include canned pumps, turbomolecular vacuum pumps, machine spindle tools, gas turbine engines, and flywheel energy storage—featuring a wide range of speed and power requirements. In [5], Clark *et al.* compare rolling element, foil, and magnetic

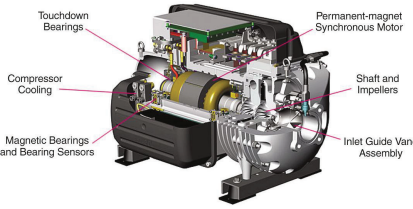


Fig. 3. 300 kW, 20,000 r/min AMB HVAC compressor [37].

bearings for engine applications (i.e. generators) and conclude that magnetic bearings are better suited for larger engines with large loads (i.e. a 10 MW machine is discussed).

In [37], Eaton *et al.* review commercial deployment of magnetic bearing technology in the petroleum and chemical industries. They highlight successful use-cases in natural gas pipeline compressors, vertical pump motors (where a 3–5% efficiency improvement is reported), subsea compressors, wastewater treatment aeration equipment, and refrigeration compressors (highlighting a 300 kW commercial HVAC chiller compressor, reproduced in Fig. 3). Two detailed case studies are presented to compare the cost, efficiency, and payback period of motor deployments with and without AMBs.

The use of magnetic levitation in HVAC chiller compressors has had an especially broad commercial impact for large enterprise-scale systems (100+ kW) with several commercially available products [37]. An example of recent commercial AMB development is described in [38] for a 450 kW, 17,000 r/min chiller compressor. Studies have shown that the lubricants of traditional compressor motor bearings leach into the refrigerant, impeding thermal transfer and thereby decreasing system efficiency in excess of 10% [39]. AMBs offer an oil-free, high efficiency solution. Magnetic bearings have also been widely commercialized for wastewater aeration compressors. Numerous reports document the benefits to municipalities of replacing legacy blower technology with direct-drive blower systems featuring non-contact bearings [7], [40]–[43]. These benefits include improved reliability, the use of high rotational speeds to decrease equipment size (increase treatment capacity within existing blower room infrastructure), and energy efficiency (legacy technology is often reported with system efficiencies under 50%). Efficiency improvement is especially important because the energy to operate the aeration blower motors constitutes approximately 25–40% of a typical wastewater treatment facility’s operating budget [40], [43]. In [44], the authors interview manufacturers, distributors, and users of wastewater blower systems to understand the motor design requirements and suitability of bearingless motors. Based on these results, bearingless design target ratings of 100 kW, > 95% efficiency, and 30,000 r/min are proposed.

III. BEARINGLESS MOTOR SOLUTIONS

By definition, bearingless motors are electromechanical devices that are able to produce either radial or axial forces (in addition to torque) to replace one or more bearings in the motor system. The remaining degrees of freedom are supported by either AMBs or some other bearing technology. Bearingless motor technology has been developed over the last several decades, with key theory summarized in two

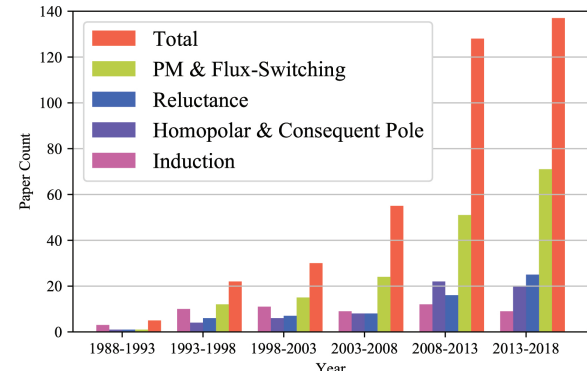


Fig. 4. Number of papers with experimental results published by year.

textbooks [45], [46]. The number of papers published with experimental results is shown in Fig. 4 and has been growing quadratically since 1988. This indicates the increased interest in and maturity of bearingless motor technology. Despite the extensive research on this technology, there has been only limited work on designing these bearingless machines for the power ratings required in large transportation and industrial applications.

Bearingless motor topologies, motor technologies, and research on large transportation and industrial bearingless motor systems are now reviewed.

A. Bearingless Motor Topologies

Bearingless motors are now categorized based on the number of degrees of freedom (DOF) that the bearingless motor can actively control.

1) *0-DOF Bearingless Motors*: It is well-known from Earnshaw’s Theorem that magnetostatic forces alone are unable to provide stable levitation. Most magnetic levitation systems are actively actuated, using feedback control. However, it is possible to create stable magnetic forces passively using the principle of electrodynamic forces—where the rotor’s rotational motion induces current in a short-circuited stator winding. It is shown in [47] that a carefully designed suspension winding can be shorted-circuited to provide suspension forces for vibration suppression, eliminating the requirement of displacement sensor, inverter and digital controller. Several recent publications have focused on extending this idea to provide complete passive magnetic levitation within a bearingless motor [48], [49]. This technology is at an early research stage, with only minimal experimental validation available, and has not yet received detailed consideration for large power applications.

2) *1-DOF Bearingless Motor*: These types of bearingless motors are typically able to create controllable axial forces. Examples in the literature include the conical aircraft in-wheel motor [33], [34] described in Section II-A and single-drive bearingless motors [50]–[52]. The single-drive bearingless motors are able to use a single three phase inverter to control both torque and axial forces, with the remaining DOF being stabilized by passive magnetic forces. This has been developed as a low cost, low power (< 30 W) technology.

3) *2-DOF Bearingless Motor*: These types of bearingless motors create radial $x-y$ forces, but are stabilized in the remaining DOF by other means. Two categories of interest to

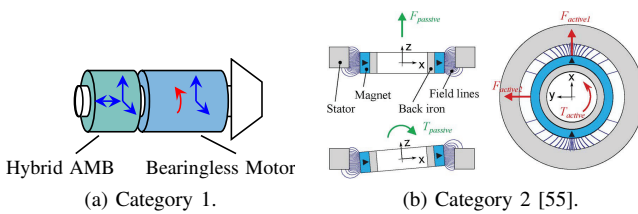


Fig. 5. 2-DOF bearingless motor topologies.

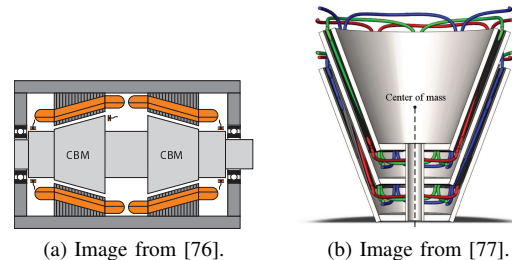


Fig. 7. 5-DOF bearingless motor topologies. CBM: Conical Bearingless Motor.

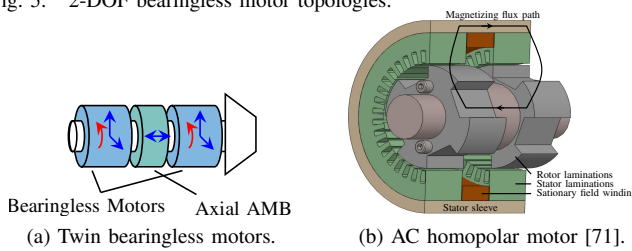


Fig. 6. 4-DOF bearingless motor topologies.

this paper: 1) bearingless motors stabilized by AMBs and 2) bearingless slice motors stabilized by passive magnetic forces. The topology for category 1) is shown in Fig. 5a, where the “hybrid AMB” is able to produce both axial and radial forces. The hybrid AMB can be replaced with separate axial and radial AMBs or with mechanical bearings. This topology has been widely developed in the literature and textbooks [45], [46] and has been considered for meeting the power requirements of large industrial motor systems [12], [13], [53], [54].

Category 2, bearingless disk or slice motors, have been developed and brought to market for centrifugal compressors and mixing devices in semiconductor, bioreactors, and medical applications—and have been the focus of many review and design papers, for example [55]–[59]. The topology along with the active and passive forces is depicted in Fig. 5b. A large rotor diameter to length ratio is required to ensure stable levitation. This restricts the topology’s power capabilities, particularly at high speeds where the material strength limits the allowable rotor diameter. Typical design power ratings are 1.2 kW or less [59], [60], but designs in the 3–4 kW range are reported in [60]–[62]. Rotational speeds range from under 500 r/min to over 100,000 r/min [55], [63].

4) 4-DOF Bearingless Motor: These systems typically consist of two bearingless motor units, each able to produce radial x - y forces, and an axial magnetic bearing. This topology is depicted in Fig. 6a and has been considered for meeting the power requirements of large industrial motor systems [44], [64]–[68]. An alternate 4-DOF topology consists of a single bearingless ac homopolar motor and one axial magnetic bearing [45], [69]–[71]. The ac homopolar motor is shown in Fig. 6b and has two rotor / stator sections, each able to create radial x - y forces. This machine works best when it has at least 8 poles, which will result in very high electric frequencies in the direct drive compressor applications (30,000 - 300,000 r/min) highlighted in Section II.

5) 5-DOF Bearingless Motor: Bearingless conical motors have been proposed which are capable of controlling radial x - y forces in two planes as well as axial forces. A typical topology is depicted in Fig. 7a. Projects include a NASA flywheel initiative with an inside-out vertical rotor [72]–[74], a 1 kW, 18,000 r/min horizontal shaft machine [75], [76], and

a nested double rotor cone motor [77] shown in Fig. 7b.

B. Motor Types For Large Bearingless Motors

Examples of bearingless versions of nearly every motor system can be found in the literature [45], [78], [79], including the following:

- induction [12], [64], [80]–[85];
- permanent magnet [13], [51], [54], [61], [65]–[68], [72]–[77], [86]–[91];
- consequent pole [92]–[95];
- synchronous reluctance [96]–[98];
- switched reluctance [99]–[102];
- ac homopolar [44], [69]–[71], [103];
- flux switching [104]–[107];
- doubly salient [108]; and hysteresis motors [109].

Of these motors, bearingless versions of the induction and permanent magnet motor have received the most attention for industrial scale power levels.

In [44], target bearingless motor system ratings for wastewater aeration compressors are proposed to be 100 kW, > 95% efficiency, and 30,000 r/min. The paper goes on to investigate the potential for a 4-DOF bearingless ac homopolar motor system to meet this criteria. Studies targeting similar ratings have been conducted by Jastrzebski *et al.* in [65]–[67] based around an inset permanent magnet motor design. In [68], a 4-DOF, 50 kW, 60,000 r/min bearingless surface mount permanent magnet motor design is investigated. In [86], a 50 kW, 9,000 r/min axial flux permanent magnet design is investigated. These papers all consist of numeric design studies and do not present experimental validation.

C. Existing Prototypes from Literature

This section reviews experimental prototype test results published in the literature as a means to assess the technology readiness of bearingless motors for medium and large power applications. The authors have conducted an exhaustive literature review going back to 1988 and the results are shown in terms of power versus motor types (Fig. 8), efficiency versus power (Fig. 9a), power versus speed (Fig. 9b), speed versus rotor diameter (Fig. 9c), and torque density versus speed (Fig. 9d). Note that only prototypes with sufficient experimental data reported are presented in the plots.

The popularity of the different motor types is shown in Fig. 8 along with the experimental measured load power. For example, for the surface mounted permanent magnet (SPM) motor, there are 21 prototypes tested below 1 kW, 5 between

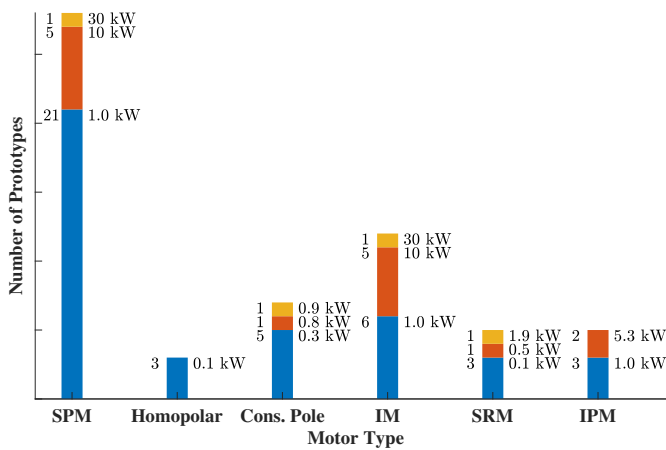


Fig. 8. Number of prototypes of different motor types. SPM: Surface Mounted Permanent Magnet; IM: Induction Motor; SRM: Switched Reluctance Motor; IPM: Interior Permanent Magnet. All data corresponds to prototypes where the magnetic suspension provides complete levitation.

1–10 kW, and 1 above 10 kW. The plot indicates that SPM and induction motors are the most commonly investigated motor types for medium power ratings.

According to Fig. 9a, the highest experimental efficiency reported is above 95.9% (tested at 1.5 kW) [111]. The highest experimental power of the tested prototypes is 30 kW, including a 30 kW, 30,000 r/min, 2-DOF bearingless surface mount permanent magnet motor with a measured efficiency of 92.7% [13] and a 30 kW, 3,000 r/min canned 2-DOF bearingless induction motor pump [12]. A 30 kW, 3000 r/min bearingless induction motor with a rotor supported by contact bearings has been developed in [80], [81], where the bearingless motor forces are used to dampen vibrations (not shown in Fig. 9 because it is not fully levitated). There are currently no examples of bearingless motor technology being tested within the 100 kW, > 95% efficiency target performance goals for industrial applications (“Desired range” label in Fig. 9a).

Fig. 9b benchmarks speed and power test data of bearingless motors against limits in high speed, high performance electric machines. The capabilities of high speed, high performance machines (with conventional bearings) are extracted from [110] and displayed as a set of “r/min $\times \sqrt{\text{kW}}$ ” lines in Fig. 9b for different motor types. These lines are used in high speed motor literature [110], [112] to represent limits on the achievable power rating of different motor types due to the mechanical design (primarily rotor dynamics, structural integrity, and bearing limitations). Current bearingless motor prototype test data are well short of these benchmarks, indicating that designs are not realizing the full potential of electric machines.

In Fig. 9c, bearingless motor prototypes are categorized using experimental tip speed. A similar plot was provided in [113], which only considered slice motors. Fig. 9c extends this presentation to also include shafted motors as this is most applicable to medium and high power applications. High speed motors are usually designed to have a tip speed greater than 100 m/s [114]. In Fig. 9c, only permanent magnet motors and homopolar motors are tested above 100 m/s tip speed range. Induction motors are popular solutions for non-bearingless high speed machines and can reach a tip speed of 400 m/s

with a solid rotor [110]. However, the bearingless version of the induction motor is tested far below 50 m/s. This is likely because typical high strength induction motor rotor structures (solid/slotted rotors) cannot be used due to excessive losses caused by the suspension field at high speeds [115].

Fig. 9d shows the prototypes in terms of experimental torque per rotor volume versus speed. Torque per rotor volume is a standard performance metric that is related to motor power density and average magnetic shear stress, discussed in Section IV-B and (9), and reflects the utilization level of magnetic materials for torque production. Only torque data points that were experimentally measured (instead of the reported design values) are shown. According to [116], high performance servo motors have a torque per rotor volume value ranging from 15 to 50 kNm/m³. Several bearingless prototypes are within or even exceed this range, all below 15,000 r/min.

Based on the prototypes reported from the literature, one concludes that current bearingless motor technology does not yet compare well with conventional motor technology for industrial applications. This is primarily observed in the low efficiency and power ratings (≤ 30 kW) of the experimental data in Fig. 9. Since many bearingless motor prototypes exhibit a high torque per rotor volume (indicating effective use of the magnetic materials), this suggests that the limitations in power rating may be due to challenges with the mechanical design. This includes 1) the inability to use solid rotors in induction motors and 2) bearingless SPM motors likely requiring a smaller effective airgap to create sufficient suspension forces (see the force sizing equations presented later in Table I), which will mandate a thinner magnet retaining sleeve that may be unable to support high centrifugal loading. Another possible explanation for the relatively lower power ratings is that the low efficiency numbers reported in Fig. 9a make current bearingless technology uninteresting for high power applications, where efficiency is critical.

D. Challenges and Advancements

Challenges and opportunities lie in the development and experimental validation of a high efficiency, large bearingless motor system. This includes careful design optimization to simultaneously achieve high power ratings (on the order of 100 kW), high efficiency (> 95%), and suitable levitation performance. The bearingless motor design optimization is significantly more constrained than a standard motor design due to stringent levitation performance requirements. For example, [66] discusses limitations on the allowable error angle of the suspension force vector—which is analogous to torque ripple. In bearingless permanent magnet motor designs, a trade-off exists in the thickness of the permanent magnets between torque rating and suspension rating. In bearingless induction motor designs, care must be taken to prevent the squirrel cage rotor from reacting to the suspension winding field and creating force disturbances—a phenomenon that has been demonstrated to worsen with increasing loads [45], [64], [83], [115]. Finally, studies are needed on the complete optimization of bearingless motor design, including the use of an optimization algorithm with computationally efficient

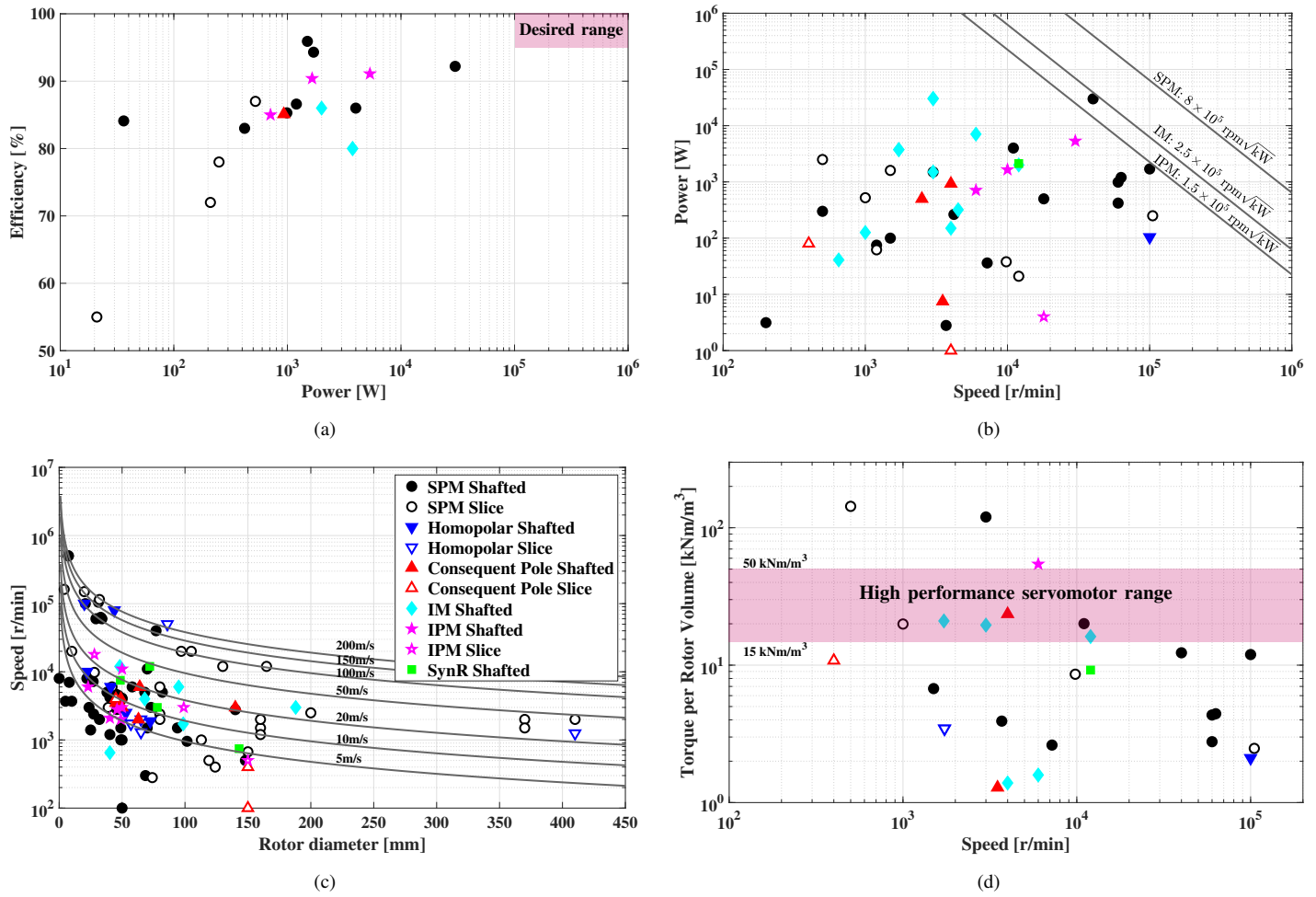


Fig. 9. Summary of published bearingless motor test data. In (a) and (d), shaded regions indicate desired performance range for industrial applications; in (b) three reference lines indicate power-speed capability of non-bearingless motors reported in [110]; in (c) the solid lines indicate rotor surface speeds (m/s).

modeling techniques. Preliminary investigations into this are beginning to appear in the literature, i.e. [115], [117].

A promising recent advancement for the development of large bearingless motors is the combined winding. These windings use the same coils to create torque and levitation force. This removes a design trade-off in slot space allocation between the torque and suspension windings—25%–40% of the slot space is often allocated to the suspension winding as a safety margin [13], [75], [118], [119], while during normal operating conditions < 5% of the slot space is needed by the suspension winding [120], [121]. By using a combined winding, the bearingless motor drive is able to dynamically allocate slot space to levitation or torque purposes during runtime. There is a large volume of literature published on combined windings, key papers include [113], [122]–[128]. Combined windings have been shown to yield significant torque density and efficiency improvements in the electric machine. For example, 30–40% copper loss reduction is reported in [124]. Typical implementations of combined windings pose challenges for the power electronics of the bearingless motor drive related to the required number of components, voltage/current rating of the devices, and cross-coupling between suspension and torque operation [129], [130]. Additional research is needed

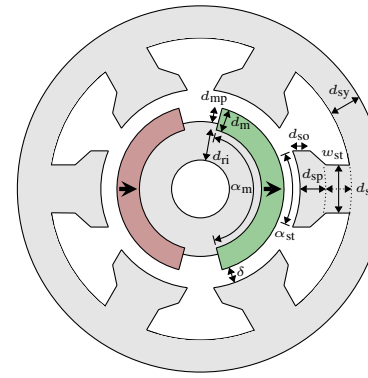


Fig. 10. Permanent magnet motor geometric parameterization used for optimization. Note that the optimized design has 24 slots.

on bearingless motor drives for combined windings to realize the full performance potential of bearingless motor systems.

E. Feasibility Study of Industrial-Scale Bearingless Motors

A study is now presented to show the potential for bearingless motors to meet the requirements of industrial applications. Separate and combined windings are compared for two

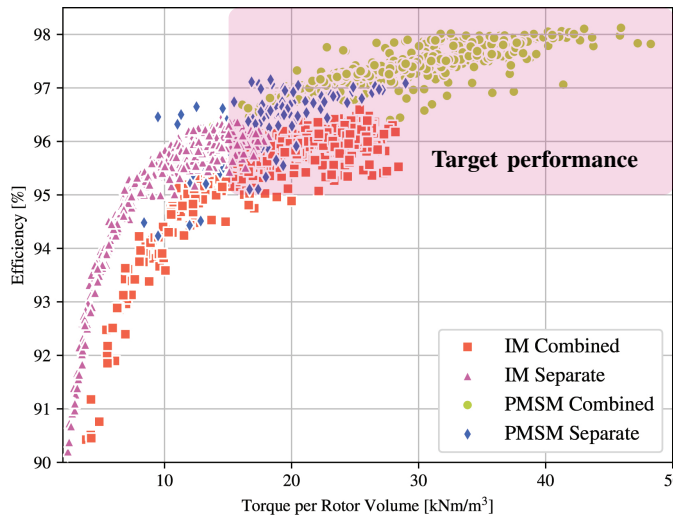


Fig. 11. Efficiency versus torque density plot for 100 kW, 30,000 r/min bearingless motor designs obtained from the optimization. Each point represents a single design that has force error angle (E_a) less than 10 deg.

bearingless motor types, an induction motor and a permanent magnet motor. The optimization procedure and the geometric parameterization used for the induction motor is described in [120]. This procedure is adapted for the permanent magnet motor (surface-mounted N40H magnets with a carbon fiber retaining sleeve) using the parameterization shown in Fig. 10. Three design objectives are used for the induction motor: torque per rotor volume, efficiency, and force/torque ripple performance [120]. The permanent magnet optimization uses these same objectives with the exception that the torque per rotor volume objective is changed to active material cost. For both designs, the stator slot number $Q_s = 24$, motor pole pair number $p = 1$, stator current density $J_s = 4$ Arms/mm², and stator slot packing factor $k_p = 0.5$.

Fig. 11 shows the optimization results in terms of motor efficiency versus torque density. Since the results are obtained using Pareto non-dominated sorting, they should be interpreted using the concept of Pareto dominance.¹ Designs using separated windings are dominated by the designs using combined windings, and induction motor design is dominated by permanent magnet motor design. Fig. 11 shows the potential to use advanced optimization techniques and combined windings to improve both the bearingless induction and permanent magnet motors to meet 1) the 95%+ efficiency required for direct drive compressors mentioned earlier [44] and 2) the torque density expected from high performance servo motors.

IV. DESIGN SIZING

This section derives design sizing equations for bearingless motors. In electric motor sizing, the torque rating is traditionally related to fundamental properties of the machine design: electric loading (linear current density), magnetic loading (airgap magnetizing field), and the volume of the rotor. Since each of these quantities are constrained by separate physics

¹Pareto dominance: a point P1 is said to dominate another point P2, if all of P1's objectives are no worse than P2's and at least one of P1's objectives is better than that of P2's.

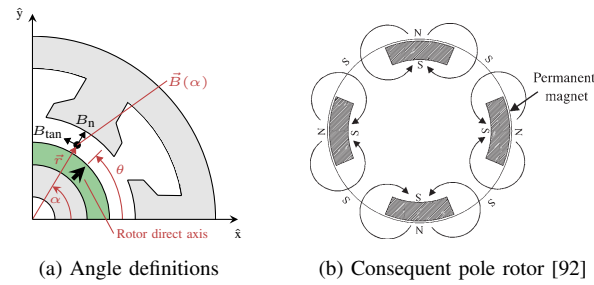


Fig. 12. Design sizing figures.

TABLE I
FORCE SIZING EQUATIONS FOR BEARINGLESS MOTOR CATEGORIES

	$p_s = p \pm 1$	Cons. Pole	AC Homopolar
$\frac{F_{\text{Rated}}}{V_R}$	$\sigma_S \left(\frac{1}{p_s \delta_e} \pm \frac{1}{r} \right)$	$\sigma_S g_2$	$2 [g_1 + 1/r] \sigma_S g_0$ $+ g_2 \sigma_S$
$\left \frac{F_{\text{Maxwell}}}{F_{\text{Lorentz}}} \right $	$\frac{r}{p_s \delta_e}$	-	$\left(g_1 + \frac{g_2}{2} \frac{\dot{B}_m}{B_{m0}} \right) r$

of the machine, this type of analysis allows the designer to make a preliminary evaluation of a machine design for any given specification (power and speed rating) based on technology constraints (material limits and cooling capabilities). This section extends this approach to determine the suspension force rating of different bearingless motors. The results are summarized in Table I. These results are related to the empirical observations of Section III-C and will be useful to bearingless machine designers as both a preliminary step in the design process (obtaining approximate dimensions) and in determining which bearingless motor technology is most appropriate for a given application.

This section first establishes the simple modeling framework used to derive the sizing laws, the well-known motor sizing laws are then summarized, and finally the bearingless motor force sizing laws are derived.

A. Analytic Modeling Framework

Bearingless motors are modeled as having two stator windings, each with a different number of pole pairs: p pole-pairs for the torque winding, p_s pole-pairs for the suspension winding. Combined winding bearingless motors can be modeled as having these two separate windings for design sizing purposes. Using the standard assumption of infinite permeability in the iron, the winding currents can be considered as an equivalent linear current density $A(\alpha)$ on the inner bore of the stator

$$A(\alpha) = \hat{A} \sin(n\alpha - \psi) \quad (1)$$

where \hat{A} is the “electric loading” of a machine. Standard values for electric loading are well-known in the literature and are typically limited by the cooling system of the machine [131]. When (1) is referring to the motor winding, $\hat{A} = \hat{A}_T$ and $n = p$ pole-pairs. When (1) is referring to the suspension winding, $\hat{A} = \hat{A}_S$ and $n = p_s$ pole-pairs. The angle ψ is determined by the phase angle of the winding currents.

With a centered rotor and an airgap effective length of δ_e assumed, this linear current density results in normal (2) and

tangential (3) airgap fields, depicted in Fig. 12a.

$$B_{n,w}(\alpha) = \mu_0 \frac{r\hat{A}}{n\delta_e} \cos(n\alpha - \psi) \quad (2)$$

$$B_{tan,w}(\alpha) = -\mu_0 A(\alpha) \quad (3)$$

Here, r is the airgap radius and μ_0 is the permeability of air. In addition, the motor contains a normal magnetizing field:

$$B_{n,m}(\alpha) = \hat{B}_m \cos(p\alpha - \theta) \quad (4)$$

The total airgap field is the summation of the winding fields and the magnetizing field. The Maxwell stress tensor can be used to find the stress acting on the rotor's surface as

$$\vec{\sigma} = \begin{bmatrix} \sigma_n \\ \sigma_{tan} \end{bmatrix} = \begin{bmatrix} \frac{1}{2\mu_0} (B_n^2 - B_{tan}^2) \\ \frac{1}{\mu_0} B_n B_{tan} \end{bmatrix} \quad (5)$$

where the subscripts “n” and “tan” indicate normal and tangential stress components in the same directions as indicated for the fields in Fig. 12a. The σ_n stress component is frequently referred to in the literature as producing Maxwell forces and the σ_{tan} component as producing Lorentz forces. These stresses can be integrated over the rotor's airgap surface S to find the torque T and forces F_x or F_y acting upon the rotor:

$$T = \int_S \vec{r} \times \vec{\sigma} dS \quad (6)$$

$$\begin{bmatrix} F_x \\ F_y \end{bmatrix} = \begin{bmatrix} \int_S \vec{\sigma} \cdot \hat{x} dS \\ \int_S \vec{\sigma} \cdot \hat{y} dS \end{bmatrix} \quad (7)$$

where \hat{x} , \hat{y} , and \vec{r} are depicted in Fig. 12a.

B. Traditional Motor Sizing Law

The well-known motor sizing law (8) can be derived by evaluating (6) when (1) is configured as a motor winding.

$$T = 2 \langle \sigma_{tan} \rangle V_R \quad (8)$$

Here, $\langle \sigma_{tan} \rangle$ is the average shear stress (9) and $V_R = \pi r^2 l$ is the rotor volume with active length l and airgap radius r .

$$\langle \sigma_{tan} \rangle = \frac{\hat{B}_m \hat{A}_T}{2} \quad (9)$$

The rotor's radius and length can be scaled within constraints placed on 1) the radius by the rotor's structural integrity (rotational speed combined with material strength) and 2) the rotor's length by rotor dynamics. Common values for the magnetic and electric loading (\hat{B}_m and \hat{A}_T) are in the range of 0.7 - 1.05 T and 30 - 80 kA/m (air cooled) [131] based on the motor type (induction, permanent magnet, etc.), thermal design, and type of magnetic steel. It can be seen from (8) that the torque per rotor volume (T/V_R) metric identified in Section III-C (see Fig. 9d) is the product of the magnetic and electric loading, and therefore a fundamental indicator of the electromagnetic performance of a motor design. The power speed trends in Fig. 9b additionally reflect the mechanical design of the rotor's active length and diameter.

C. Force sizing law for $p_s = p \pm 1$ bearingless motors

Conventional motors (i.e., induction and permanent magnet motors) can be transformed into bearingless motors by adding a suspension winding with $p_s = p \pm 1$ pole pairs. Design sizing equations are derived for the suspension forces by evaluating (7) with $\hat{A} = \hat{A}_S$, $\psi = \theta + \phi_S$, and $n = p_s$ as (10).

$$\begin{bmatrix} F_x \\ F_y \end{bmatrix} = \sigma_S V_R \left(\frac{1}{p_s \delta_e} \pm \frac{1}{r} \right) \begin{bmatrix} \cos \phi_S \\ \pm \sin \phi_S \end{bmatrix} \quad (10)$$

$$\sigma_S = \frac{\hat{B}_m \hat{A}_S}{2} \quad (11)$$

In this expression, σ_S does not have the same physical meaning as $\langle \sigma_{tan} \rangle$ (9), but is defined in a similar manner in terms of the magnetic and electric loading. This is done so that the force sizing law can be compared to the torque sizing law (8). Forces in the \hat{x} and \hat{y} directions are controlled by ϕ_S (the phase angle of the suspension currents). This can be viewed in a field oriented control reference frame as d and q currents and is well documented in the literature [45].

The $\frac{1}{p_s \delta_e}$ term of (10) corresponds to the Maxwell forces, which increase with lower p_s and δ_e values. The $\pm \frac{1}{r}$ term of (10) corresponds to the Lorentz forces and adds to the Maxwell forces for designs with $p_s = p + 1$, while subtracting from the Maxwell forces for designs with $p_s = p - 1$. Notice that Maxwell forces decrease in $p_s = p + 1$ designs, while Lorentz forces increase. The Maxwell force scales with the machine dimensions and electric and magnetic loading in the same manner as the machine's torque rating, while the Lorentz force is less sensitive to the rotor's radius. The ratio of Maxwell and Lorentz force components is given as follows

$$\left| \frac{F_{\text{Maxwell}}}{F_{\text{Lorentz}}} \right| = \frac{r}{p_s \delta_e} \quad (12)$$

In most designs, this ratio is $\gg 1$ and Lorentz forces are neglected. However, there are a class of bearingless motors which rely on Lorentz forces instead of Maxwell forces [132], [46], [77], [86], [90], [91]. These designs typically require very large airgap length or no rotor/stator iron. The relative force magnitudes are described in more detail in [133].

Producing a constant radial force requires that the suspension field rotates at a speed of ω_s/p_s , where ω_s is the synchronous frequency of the motor. This can be viewed in induction motor terms as a slip of $1/p$, and has a frequency of ω_s/p in the rotor's reference frame [13], [88]. This rotating field causes iron losses in the rotor. Examples of the design process for relevant $p_s = p \pm 1$ bearingless motors are presented in [87], [134].

D. Force sizing law for $p_s = 1, p \geq 4$ bearingless motors

Another popular class of bearingless motors have the properties that $p_s = 1$ and $p \geq 4$. This class consists of the bearingless ac homopolar motor and consequent pole motor, shown in Fig. 6b and 12b, and has the advantageous property of suspension forces being independent of the rotor's angular location. This means that rotational position sensing is not needed to obtain stable levitation. For these motors, the

effective airgap length δ_e is modeled as (13). The airgap field expression (2) is then modified by replacing δ_e with (13).

$$\delta_e(\alpha) = \frac{1}{g_1 + g_2 \cos(p\alpha - \theta)} \quad (13)$$

1) Bearingless Consequent Pole Motor: The consequent pole motor has the same circumferential fields as (3) and fundamental magnetizing airgap field as (4). The suspension current density parameters are $n = p_s = 1$ and $\psi = \phi_S$. The force integral (7) is evaluated with these fields to derive the suspension force sizing equations (14).

$$\begin{bmatrix} F_x \\ F_y \end{bmatrix} = \sigma_S V_R g_2 \begin{bmatrix} \cos \phi_S \\ \sin \phi_S \end{bmatrix} \quad (14)$$

The consequent pole motor size scales very similar to the $p_s = p \pm 1$ bearingless motors, with the key difference being that the consequent pole motor does not experience Lorentz forces.

2) Bearingless AC Homopolar Motor: The bearingless ac homopolar motor is modeled in a similar fashion, but with a homopolar component \hat{B}_{m0} in the magnetizing field as specified as follows

$$B_{n,m}(\alpha) = \hat{B}_{m0} + \hat{B}_m \cos(p\alpha - \theta) \quad (15)$$

The ac homopolar motor consists of two rotor/stator sections—a “top” and “bottom” section [45], [69], [70]. The resulting force sizing equations are provided in (16) for each section of the ac homopolar, meaning that V_R is actually half the total active rotor volume.

$$\begin{bmatrix} F_x \\ F_y \end{bmatrix} = V_R \left(2 \left[g_1 + \frac{1}{r} \right] \sigma_{S0} + g_2 \sigma_S \right) \begin{bmatrix} \cos \phi_S \\ \sin \phi_S \end{bmatrix} \quad (16)$$

$$\sigma_{S0} = \frac{\hat{B}_{m0} \hat{A}_S}{2} \quad (17)$$

The suspension forces scale similarly to the bearingless consequent pole motor (the g_2 term) but an additional term related to the homopolar field (the σ_{S0} term) is present. Note also the presence of Lorentz forces (the $\frac{1}{r_g}$ term). The ratio of Maxwell to Lorentz force components can be calculated as

$$\left| \frac{F_{\text{Maxwell}}}{F_{\text{Lorentz}}} \right| = \left(g_1 + \frac{g_2}{2} \frac{\hat{B}_m}{\hat{B}_{m0}} \right) r \quad (18)$$

As in the case of $p_s = p \pm 1$ bearingless motors, this ratio is typically $\gg 1$ and Lorentz forces are often neglected.

The same torque sizing equation (8) can be applied to the ac homopolar motor, but when scaling the geometric dimensions, saturation in the axial flux paths must be considered [135].

V. CONCLUSION

Potential use-cases for bearingless motors in large transportation and industrial systems have been reviewed. Bearingless motors have potential to decrease the cost and size of magnetic suspension systems, thereby allowing new application spaces to benefit from the high efficiency and intelligent operation of magnetic levitation. Relevant literature on developing large bearingless motor systems has been reviewed. It was shown that this technology needs additional development to reach the power ratings required in transportation and industrial applications. Finally, design sizing equations have been presented to compare different bearingless motor technologies.

REFERENCES

- [1] A. Morya, M. Moosavi, M. C. Gardner, and H. A. Toliyat, “Applications of wide bandgap (wbg) devices in ac electric drives: A technology status review,” in *Electric Machines and Drives Conference (IEMDC), 2017 IEEE International*. IEEE, 2017, pp. 1–8.
- [2] D. Han, Y. Li, and B. Sarlioglu, “Analysis of sic based power electronic inverters for high speed machines,” in *Applied Power Electronics Conference and Exposition (APEC), 2015 IEEE*. IEEE, 2015, pp. 304–310.
- [3] S. Li, Y. Li, W. Choi, and B. Sarlioglu, “High-speed electric machines: Challenges and design considerations,” *IEEE Transactions on Transportation Electrification*, vol. 2, no. 1, pp. 2–13, 2016.
- [4] A. Borisavljevic, *Limits, modeling and design of high-speed permanent magnet machines*. Springer Science & Business Media, 2012.
- [5] D. J. Clark, M. J. Jansen, and G. T. Montague, “An overview of magnetic bearing technology for gas turbine engines,” 2004.
- [6] C. Gong, S. Li, and T. Haberle, “Practical considerations in the design and manufacture of ultra-high speed switched reluctance machines over 1 million rpm,” in *2019 IEEE International Electric Machines & Drives Conference (IEMDC)*. IEEE, 2019, pp. 25–30.
- [7] A. Irving and J. Ibets, “High-speed bearing technologies for wastewater treatment applications,” *Proceedings of the Water Environment Federation*, vol. 2013, no. 20, pp. 98–106, 2013.
- [8] C. DellaCorte and R. J. Bruckner, “Remaining technical challenges and future plans for oil-free turbomachinery,” *Journal of Engineering for Gas Turbines and Power*, vol. 133, no. 4, p. 042502, 2011.
- [9] C. DellaCorte, K. C. Radil, R. J. Bruckner, and S. A. Howard, “Design, fabrication, and performance of open source generation i and ii compliant hydrodynamic gas foil bearings,” *Tribology transactions*, vol. 51, no. 3, pp. 254–264, 2008.
- [10] C. Teo, L. Liu, H. Li, L. Ho, S. Jacobson, F. Ehrich, A. Epstein, and Z. Spakovsky, “High-speed operation of a gas-bearing supported mems-air turbine,” *Journal of Tribology*, vol. 131, no. 3, p. 032001, 2009.
- [11] E. L. Severson, “Bearingless motor technology for industrial and transportation applications,” in *2018 IEEE Transportation Electrification Conference and Expo (ITEC)*. IEEE, 2018, pp. 266–273.
- [12] C. Redemann, P. Meuter, A. Ramella, and T. Gempp, “30kw bearingless canned motor pump on the test bed,” in *Seventh International Symp. on Magnetic Bearings, August 23-25, 2000, ETH Zurich*, 2000.
- [13] G. Munteanu, A. Binder, and T. Schneider, “Loss measurement of a 40 kw high-speed bearingless pm synchronous motor,” in *2011 IEEE Energy Conversion Congress and Exposition*. IEEE, 2011, pp. 722–729.
- [14] R. John, J. W. Long, H. T. Massey, B. P. Griffith, B. C. Sun, A. J. Tector, O. H. Frazier, and L. D. Joyce, “Outcomes of a multicenter trial of the levitronix centrimag ventricular assist system for short-term circulatory support,” *The Journal of thoracic and cardiovascular surgery*, vol. 141, no. 4, pp. 932–939, 2011.
- [15] Levitronix, “Maglev pump tank mixer system ptm-2000 pumping and mixing with one single device,” Sep. 2015.
- [16] Celeroton, “Cm-amb-400: High-speed active magnetic bearing motor for direct drive of applications with highest speeds.” Jun. 2017.
- [17] R. Pili, A. Romagnoli, K. Kamossa, A. Schuster, H. Spliethoff, and C. Wieland, “Organic rankine cycles (orc) for mobile applications—economic feasibility in different transportation sectors,” *Applied Energy*, vol. 204, pp. 1188–1197, 2017.
- [18] L. A. Hawkins, L. Zhu, and E. J. Blumber, “Development of a 125 kw amb expander/generator for waste heat recovery,” *Journal of Engineering for Gas Turbines and Power*, vol. 133, no. 7, p. 072503, 2011.
- [19] Calnetix technologies organic rankine cycle systems. Accessed: 2018-04-26. [Online]. Available: <https://www.calnetix.com/organic-rankine-cycle-systems/>
- [20] G. Schweitzer, “Active magnetic bearings-chances and limitations,” in *IUTAM Sixth International Conference on Rotor Dynamics, Sydney, Australia*, vol. 1. Citeseer, 2002, pp. 1–14.
- [21] R. Quigley, “More electric aircraft,” in *Applied Power Electronics Conference and Exposition, 1993. APEC'93. Conference Proceedings 1993., Eighth Annual*. IEEE, 1993, pp. 906–911.
- [22] M. Andres, T. Temple, and T. Coons, “Permanent magnet turbo-generator having magnetic bearings,” Aug. 19 2003, uS Patent 6,608,418.
- [23] J. P. Lyons and M. A. Preston, “Fault tolerant active magnetic bearing electric system,” Nov. 26 1996, uS Patent 5,578,880.

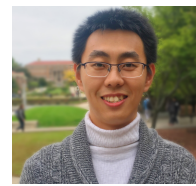
- [24] T. Noguchi and T. Wada, "1.5-kw, 150,000-r/min ultra high-speed pm motor fed by 12-v power supply for automotive supercharger," in *2009 13th European Conference on Power Electronics and Applications*. IEEE, 2009, pp. 1–10.
- [25] Y. Yamashita, S. Ibaraki, K. Sumida, M. Ebisu, B. An, and H. Ogita, "Development of electric supercharger to facilitate the downsizing of automobile engines," *Mitsubishi Heavy Industries Technical Review*, vol. 47, no. 4, pp. 7–12, 2010.
- [26] W. Lee, E. Schubert, Y. Li, S. Li, D. Bobba, and B. Sarlioglu, "Overview of electric turbocharger and supercharger for downsized internal combustion engines," *IEEE Transactions on Transportation Electrification*, vol. 3, no. 1, pp. 36–47, 2017.
- [27] J.-W. Jaissle, "Turbocharger with magnetic bearing system that includes dampers," Jan. 25 2005, uS Patent 6,846,167.
- [28] J. K. Fremerey, M. Lang, and J.-W. Jaissle, "Exhaust gas turbocharger," Aug. 1 2006, uS Patent 7,082,763.
- [29] R. S. Lerosen, "Electromagnetic and air bearing combination for turbocharger shaft and wheel balance measurement machines," Dec. 22 2015, uS Patent 9,217,330.
- [30] J. Da Silva, Y. Dupuis, O. Lemarchand, L. Ramdane, E. Salahun, and U. Schroeder, "Hybrid magnetic suspension of a rotor," Jan. 9 2018, uS Patent 9,863,431.
- [31] L. Ramdane, J. Da Silva, E. Helene, F. Ponson, and U. Schroeder, "Electric centrifugal compressor for vehicles," Dec. 26 2013, uS Patent App. 13/925,390.
- [32] H. L. Adams III and H. V. Quackenboss, "Electric supercharger," Jun. 17 1997, uS Patent 5,638,796.
- [33] S. Roggia, F. Cupertino, C. Gerada, and M. Galea, "A two-degrees-of-freedom system for wheel traction applications," *IEEE Transactions on Industrial Electronics*, vol. 65, no. 6, pp. 4483–4491, 2018.
- [34] ——, "Axial position estimation of conical shaped motors for aerospace traction applications," *IEEE Transactions on Industry Applications*, vol. 53, no. 6, pp. 5405–5414, 2017.
- [35] C. R. Knospe, "Active magnetic bearings for machining applications," *Control Engineering Practice*, vol. 15, no. 3, pp. 307–313, 2007.
- [36] M. Kasarda, "An overview of active magnetic bearing technology and applications," *The shock and vibration digest*, vol. 32, no. 2, pp. 91–99, 2000.
- [37] D. Eaton, J. Rama, and S. Singhal, "Magnetic bearing applications & economics," in *Petroleum and chemical industry conference (PCIC), 2010 record of conference papers industry applications society 57th annual*. IEEE, 2010, pp. 1–9.
- [38] Y. Nakazawa, Y. Irino, A. Sakawaki, and K. Ohyama, "Higher radial suspension force of magnetic bearing on centrifugal compressor for hvac," in *2018 International Power Electronics Conference (IPEC-Niigata 2018-ECCE Asia)*. IEEE, 2018, pp. 244–249.
- [39] M. Key, "The high cost of ignoring chiller oil buildup," *RSES Journal*, pp. 1–4, Nov. 2002.
- [40] State and Local Climate and Energy Program, "Energy efficiency in water and wastewater facilities: A guide to developing and implementing greenhouse gas reduction programs," U.S. Environmental Protection Agency (EPA), Tech. Rep., 2013.
- [41] B. Mumy, A. Bahar, R. Welsh, D. Bauer, and D. Handley, "Embracing variety: Cincinnati's experience with maximizing aeration system energy efficiency at three facilities," *Water Environment Federation Magazine*, pp. 75 – 78, December 2014.
- [42] W. Schilling and A. Turriciano, "Paying for themselves, an evaluation of turbo blower life-cycle costs," *Proceedings of the Water Environment Federation*, vol. 2011, no. 15, pp. 2138–2148, 2011.
- [43] Office of Wastewater Management, "Evaluation of energy conservation measures for wastewater treatment facilities," U.S. Environmental Protection Agency (EPA), Tech. Rep., September 2010.
- [44] E. Severson and N. Mohan, "Bearingless motor system design for industrial applications," in *Electric Machines and Drives Conference (IEMDC), 2017 IEEE International*. IEEE, 2017, pp. 1–8.
- [45] A. Chiba, T. Fukao, O. Ichikawa, M. Oshima, M. Takemoto, and D. Dorrell, *Magnetic Bearings and Bearingless Drives*. Newnes, 2005.
- [46] G. Schweitzer and E. H. Maslen, *Magnetic bearings: theory, design, and application to rotating machinery*. Springer, 2009.
- [47] A. Chiba, T. Fukao, and M. A. Rahman, "Vibration suppression of a flexible shaft with a simplified bearingless induction motor drive," *IEEE Transactions on Industry Applications*, vol. 44, no. 3, pp. 745–752, May 2008.
- [48] V. Kluykens, C. Dumont, and B. Dehez, "Description of an electrodynamic self-bearing permanent magnet machine," *IEEE Transactions on Magnetics*, vol. 53, no. 1, pp. 1–9, Jan 2017.
- [49] J. Van Verdeghem, M. Lefebvre, V. Kluykens, and B. Dehez, "Dynamical modeling of passively levitated electrodynamic thrust self-bearing machines," *IEEE Transactions on Industry Applications*, vol. 55, no. 2, pp. 1447–1460, March 2019.
- [50] J. Asama, Y. Hamasaki, T. Oiwa, and A. Chiba, "Proposal and analysis of a novel single-drive bearingless motor," *Industrial Electronics, IEEE Transactions on*, vol. 60, no. 1, pp. 129–138, Jan 2013.
- [51] H. Sugimoto, S. Tanaka, A. Chiba, and J. Asama, "Principle of a novel single-drive bearingless motor with cylindrical radial gap," *Industry Applications, IEEE Trans on*, vol. 51, no. 5, pp. 3696–3706, Sept 2015.
- [52] Q. D. Nguyen and S. Ueno, "Modeling and control of salient-pole permanent magnet axial-gap self-bearing motor," *IEEE/Asme Transactions on mechatronics*, vol. 16, no. 3, pp. 518–526, 2010.
- [53] G. Munteanu, A. Binder, and T. Schneider, "Development and test of high-speed bearingless pm synchronous machines," *e & i Elektrotechnik und Informationstechnik*, vol. 128, no. 3, pp. 75–80, 2011.
- [54] G. Munteanu, A. Binder, T. Schneider, and B. Funieru, "No-load tests of a 40 kw high-speed bearingless permanent magnet synchronous motor," in *Power Electronics Electrical Drives Automation and Motion (SPEEDAM), 2010 International Symposium on*. IEEE, 2010, pp. 1460–1465.
- [55] H. Mitterhofer, W. Gruber, and W. Amrhein, "On the high speed capacity of bearingless drives," *Industrial Electronics, IEEE Transactions on*, vol. 61, no. 6, pp. 3119–3126, June 2014.
- [56] S. Silber, W. Amrhein, P. Bosch, R. Schob, and N. Barletta, "Design aspects of bearingless slice motors," *IEEE/ASME transactions on mechatronics*, vol. 10, no. 6, pp. 611–617, 2005.
- [57] T. Nussbaumer, P. Karutz, F. Zurcher, and J. W. Kolar, "Magnetically levitated slice motors—an overview," *IEEE Transactions on Industry Applications*, vol. 47, no. 2, pp. 754–766, 2011.
- [58] W. Gruber, "Bearingless slice motors: General overview and the special case of novel magnet-free rotors," in *Innovative Small Drives and Micro-Motor Systems, 2013. 9. GMM/ETG Symposium*. VDE, 2013, pp. 1–6.
- [59] M. T. Bartholet, T. Nussbaumer, S. Silber, and J. W. Kolar, "Comparative evaluation of polyphase bearingless slice motors for fluid-handling applications," *IEEE Transactions on Industry Applications*, vol. 45, no. 5, pp. 1821–1830, 2009.
- [60] P. Bösch and N. Barletta, "High power bearingless slice motor (3-4kw) for bearingless canned pumps," in *9th International Symposium on Magnetic Bearings*, Lexington, Kentucky, USA, 2004.
- [61] Q. Li, P. Boesch, M. Haefliger, J. W. Kolar, and D. Xu, "Basic characteristics of a 4kw permanent-magnet type bearingless slice motor for centrifugal pump system," in *Electrical Machines and Systems, 2008. ICEMS 2008. International Conference on*. IEEE, 2008, pp. 3037–3042.
- [62] W. Gruber, T. Nussbaumer, H. Grabner, and W. Amrhein, "Wide air gap and large-scale bearingless segment motor with six stator elements," *Magnetics, IEEE Trans on*, vol. 46, no. 6, pp. 2438–2441, June 2010.
- [63] E. Gobi, W. Amrhein, and H. Mitterhofer, "Slotless bearingless high speed disk drive designed for speeds beyond 100krpm," in *Power Electronics and Drive Systems (PEDS), 2017 IEEE 12th International Conference on*. IEEE, 2017, pp. 1–017.
- [64] M. Ohsawa, "Study of the induction type bearingless motor," in *Seventh International Symp. on Magnetic Bearings (ISMB)*, 2000, pp. 389–394.
- [65] R. P. Jastrzebski, P. Jaatinen, A. Chiba, and O. Pyrhnen, "Efficiency of buried permanent magnet type 5kw and 50kw high-speed bearingless motors with 4-pole motor windings and 2-pole suspension windings," in *The 15th International Symposium on Magnetic Bearings (ISMB15)*, Aug 2016, pp. 1–8.
- [66] R. P. Jastrzebski, P. Jaatinen, H. Sugimoto, O. Pyrhnen, and A. Chiba, "Design of a bearingless 100 kw electric motor for high-speed applications," in *Electrical Machines and Systems (ICEMS), 2015 18th International Conference on*, Oct 2015, pp. 2008–2014.
- [67] R. P. Jastrzebski, P. Jaatinen, O. Pyrhonen, and A. Chiba, "Design of 6-slot inset pm bearingless motor for high-speed and higher than 100kw applications," in *Electric Machines and Drives Conference (IEMDC), 2017 IEEE International*. IEEE, 2017, pp. 1–6.
- [68] Y. Fu, M. Takemoto, S. Ogasawara, and K. Orikawa, "Investigation of a high speed and high power density bearingless motor with neodymium bonded magnet," in *Electric Machines and Drives Conference (IEMDC), 2017 IEEE International*. IEEE, 2017, pp. 1–8.
- [69] O. Ichikawa, A. Chiba, and T. Fukao, "Inherently decoupled magnetic suspension in homopolar-type bearingless motors," *Industry Applications, IEEE Transactions on*, vol. 37, no. 6, pp. 1668 –1674, nov/dec 2001.

- [70] E. Severson, R. Nilssen, T. Undeland, and N. Mohan, "Analysis of the bearingless ac homopolar motor," in *Int Conf on Electrical Machines (ICEM)*, 2012., Sep. 2012, pp. 568 – 574.
- [71] ——, "Dual purpose no voltage winding design for the bearingless ac homopolar and consequent pole motors," *Industry Applications, IEEE Transactions on*, vol. 51, no. 4, pp. 2884–2895, July 2015.
- [72] P. Kascak, R. Jansen, T. Dever, A. Nagorny, and K. Loparo, "Levitation performance of two opposed permanent magnet pole-pair separated conical bearingless motors," in *Energy Conversion Congress and Exposition (ECCE), IEEE*, 2011, pp. 1649–1656.
- [73] P. Kascak, "Fully levitated rotor magnetically suspended by two pole-pair separated conical motors," Ph.D. dissertation, Case Western University, Cleveland, OH, 2010.
- [74] P. Kascak, R. Jansen, T. Dever, A. Nagorny, and K. Loparo, "Motorizing performance of a conical pole-pair separated bearingless electric machine," in *Energytech, 2011 IEEE*. IEEE, 2011, pp. 1–6.
- [75] G. Messager and A. Binder, "Derivation of forces and force interferences in a double conical high-speed bearingless permanent magnet synchronous motor," in *2017 IEEE International Electric Machines and Drives Conference (IEMDC)*. IEEE, 2017, pp. 1–8.
- [76] G. Munteanu, A. Binder, and S. Dewenter, "Five-axis magnetic suspension with two conical air gap bearingless pm synchronous half-motors," in *Power Electronics, Electrical Drives, Automation and Motion (SPEEDAM), 2012 International Symposium on*. IEEE, 2012, pp. 1246–1251.
- [77] J. Abrahamsson, J. Ögren, and M. Hedlund, "A fully levitated cone-shaped lorentz-type self-bearing machine with skewed windings," *IEEE Transactions on Magnetics*, vol. 50, no. 9, pp. 1–9, 2014.
- [78] A. Chiba, T. Deido, T. Fukao, and M. Rahman, "An analysis of bearingless ac motors," *Energy Conversion, IEEE Transactions on*, vol. 9, no. 1, pp. 61–68, Mar 1994.
- [79] B. Liu, "Survey of bearingless motor technologies and applications," in *Mechatronics and Automation (ICMA), 2015 IEEE International Conference on*. IEEE, 2015, pp. 1983–1988.
- [80] A. Sinervo and A. Arkkio, "Rotor radial position control and its effect on the total efficiency of a bearingless induction motor with a cage rotor," *Magnetics, IEEE Transactions on*, vol. 50, no. 4, pp. 1–9, April 2014.
- [81] A. Laiho, A. Sinervo, J. Orivuori, K. Tammi, A. Arkkio, and K. Zenger, "Attenuation of harmonic rotor vibration in a cage rotor induction machine by a self-bearing force actuator," *IEEE Transactions on Magnetics*, vol. 45, no. 12, pp. 5388–5398, 2009.
- [82] A. Chiba and J. Asama, "Influence of rotor skew in induction type bearingless motor," *IEEE Transactions on Magnetics*, vol. 48, no. 11, pp. 4646–4649, 2012.
- [83] T. Hiromi, T. Katou, A. Chiba, M. A. Rahman, and T. Fukao, "A novel magnetic suspension-force compensation in bearingless induction-motor drive with squirrel-cage rotor," *IEEE Transactions on Industry Applications*, vol. 43, no. 1, pp. 66–76, 2007.
- [84] E. Rodriguez and J. Santisteban, "An improved control system for a split winding bearingless induction motor," *Industrial Electronics, IEEE Transactions on*, vol. 58, no. 8, pp. 3401–3408, Aug 2011.
- [85] A. Chiba and T. Fukao, "Optimal design of rotor circuits in induction type bearingless motors," *IEEE Transactions on Magnetics*, vol. 34, no. 4, pp. 2108–2110, 1998.
- [86] W. Geng and Z. Zhang, "Investigation of a new ironless-stator self-bearing axial flux permanent magnet motor," *IEEE Transactions on Magnetics*, vol. 52, no. 7, pp. 1–4, 2016.
- [87] G. Bergmann and A. Binder, "Design guidelines of bearingless pmsm with two separate poly-phase windings," in *Electrical Machines (ICEM), 2016 XXII International Conference on*. IEEE, 2016, pp. 2588–2594.
- [88] T. Schneider, J. Petersen, and A. Binder, "Influence of pole pair combinations on high-speed bearingless permanent magnet motor," 2008.
- [89] X. Sun, L. Chen, and Z. Yang, "Overview of bearingless permanent-magnet synchronous motors," *Industrial Electronics, IEEE Transactions on*, vol. 60, no. 12, pp. 5528–5538, Dec 2013.
- [90] L. S. Stephens and D.-G. Kim, "Force and torque characteristics for a slotless lorentz self-bearing servomotor," *IEEE Transactions on Magnetics*, vol. 38, no. 4, pp. 1764–1773, 2002.
- [91] T. Baumgartner, R. Burkart, and J. Kolar, "Analysis and design of a 300-w 500 000-r/min slotless self-bearing permanent-magnet motor," *Ind Elec, IEEE Trans on*, vol. 61, no. 8, pp. 4326–4336, Aug 2014.
- [92] J. Amemiya, A. Chiba, D. Dorrell, and T. Fukao, "Basic characteristics of a consequent-pole-type bearingless motor," *Magnetics, IEEE Transactions on*, vol. 41, no. 1, pp. 82 – 89, jan. 2005.
- [93] J. Asama, D. Kanehara, T. Oiwa, and A. Chiba, "Development of a compact centrifugal pump with a two-axis actively positioned consequent-pole bearingless motor," *Industry Applications, IEEE Transactions on*, vol. 50, no. 1, pp. 288–295, Jan 2014.
- [94] ——, "Suspension performance of a two-axis actively regulated consequent-pole bearingless motor," *Energy Conversion, IEEE Transactions on*, vol. 28, no. 4, pp. 894–901, Dec 2013.
- [95] J. Asama, M. Amada, M. Takemoto, A. Chiba, T. Fukao, and A. Rahman, "Voltage characteristics of a consequent-pole bearingless pm motor with concentrated windings," *Magnetics, IEEE Transactions on*, vol. 45, no. 6, pp. 2823 –2826, june 2009.
- [96] H. Ding, H. Zhu, and Y. Hua, "Optimization design of bearingless synchronous reluctance motor," *IEEE Transactions on Applied Superconductivity*, vol. 28, no. 3, pp. 1–5, 2018.
- [97] A. Chiba, M. Hanazawa, T. Fukao, and M. A. Rahman, "Effects of magnetic saturation on radial force of bearingless synchronous reluctance motors," *IEEE Transactions on Industry Applications*, vol. 32, no. 2, pp. 354–362, 1996.
- [98] S. E. Saarakkala, M. Sokolov, M. Hinkkanen, J. Kataja, and K. Tammi, "State-space flux-linkage control of bearingless synchronous reluctance motors," in *Energy Conversion Congress and Exposition (ECCE), 2016 IEEE*. IEEE, 2016, pp. 1–8.
- [99] F. Ahmed, D. Saikia, S. Chatterjee, H. Singh, P. Das, and K. Kalita, "Self-bearing switched reluctance motor: A review," in *Power and Energy in NERIST (ICPEN), 2012 1st International Conference on*. IEEE, 2012, pp. 1–6.
- [100] J. Zhang, H. Wang, L. Chen, C. Tan, and Y. Wang, "Multi-objective optimal design of bearingless switched reluctance motor based on multi-objective genetic particle swarm optimizer," *IEEE Transactions on Magnetics*, vol. 54, no. 1, pp. 1–13, 2018.
- [101] L. Chen and W. Hofmann, "Speed regulation technique of one bearingless 8/6 switched reluctance motor with simpler single winding structure," *IEEE Transactions on Industrial Electronics*, vol. 59, no. 6, pp. 2592–2600, 2012.
- [102] ——, "Design procedure of bearingless high-speed switched reluctance motors," in *Power Electronics Electrical Drives Automation and Motion (SPEEDAM), 2010 International Symposium on*. IEEE, 2010, pp. 1442–1447.
- [103] J. Asama, R. Natsume, H. Fukuhara, T. Oiwa, and A. Chiba, "Optimal suspension winding configuration in a homo-polar bearingless motor," *Magnetics, IEEE Transactions on*, vol. 48, no. 11, pp. 2973 –2976, nov. 2012.
- [104] W. Amrhein, W. Gruber, W. Bauer, and M. Reisinger, "Magnetic levitation systems for cost-sensitive applicationssome design aspects," *IEEE Transactions on Industry Applications*, vol. 52, no. 5, pp. 3739–3752, 2016.
- [105] C. Zhao and H. Zhu, "Design and analysis of a novel bearingless flux-switching permanent magnet motor," *IEEE Transactions on Industrial Electronics*, vol. 64, no. 8, pp. 6127–6136, 2017.
- [106] H. Jia, J. Wang, M. Cheng, W. Hua, C. Fang, and Z. Ling, "Comparison study of electromagnetic performance of bearingless flux-switching permanent-magnet motors," *IEEE Transactions on Applied Superconductivity*, vol. 26, no. 4, pp. 1–5, 2016.
- [107] Q. Ding, T. Ni, X. Wang, and Z. Deng, "Optimal winding configuration of bearingless flux-switching permanent magnet motor with stacked structure," *IEEE Transactions on Energy Conversion*, vol. 33, no. 1, pp. 78–86, 2018.
- [108] H. Jia, M. Cheng, J. Zhu, J. Cai, Y. Cao, and Z. Jia, "Design and analysis of a bearingless doubly salient permanent magnet machine," in *Electrical Machines and Systems (ICEMS), 2017 20th International Conference on*. IEEE, 2017, pp. 1–5.
- [109] M. Noh, W. Gruber, and D. L. Trumper, "Hysteresis bearingless slice motors with homopolar flux-biasing," *IEEE/ASME Transactions on Mechatronics*, vol. 22, no. 5, pp. 2308–2318, 2017.
- [110] D. Gerada, A. Mebareki, N. L. Brown, C. Gerada, A. Cavagnino, and A. Boglietti, "High-speed electrical machines: Technologies, trends, and developments," *IEEE Transactions on Industrial Electronics*, vol. 61, no. 6, pp. 2946–2959, 2014.
- [111] G. Sala, G. Valente, A. Formentini, L. Papini, D. Gerada, P. Zanchetta, A. Tani, and C. Gerada, "Space vectors and pseudoinverse matrix methods for the radial force control in bearingless multisector permanent magnet machines," *IEEE Transactions on Industrial Electronics*, vol. 65, no. 9, pp. 6912–6922, 2018.
- [112] R. Van Millingen and J. Van Millingen, "Phase shift torquemeters for gas turbine development and monitoring," in *ASME 1991 International Gas Turbine and Aeroengine Congress and Exposition*. American Society of Mechanical Engineers Digital Collection, 1991.

- [113] W. Gruber, *Bearingless Slice Motor Systems Without Permanent Magnetic Rotors*, 2017.
- [114] A. Binder and T. Schneider, "High-speed inverter-fed ac drives," in *2007 International Aegean Conference on Electrical Machines and Power Electronics*, Sep. 2007, pp. 9–16.
- [115] J. Chen and E. L. Severson, "Design and modeling of the bearingless induction motor," in *2019 IEEE International Electric Machines and Drives Conference (IEMDC)*, May 2019, pp. 1–7.
- [116] J. R. Hendershot and T. J. E. Miller, *Design of brushless permanent-magnet machines*. Motor Design Books, 2010.
- [117] R. P. Jastrzebski, P. Jaatinen, O. Pyrhönen, and A. Chiba, "Design optimization of permanent magnet bearingless motor using differential evolution," in *2018 IEEE Energy Conversion Congress and Exposition (ECCE)*. IEEE, 2018, pp. 2327–2334.
- [118] T. Matsuzaki, M. Takemoto, S. Ogasawara, S. Ota, K. Oi, and D. Matsuhashi, "Operational characteristics of an ipm-type bearingless motor with 2-pole motor windings and 4-pole suspension windings," *IEEE Transactions on Industry Applications*, vol. 53, no. 6, pp. 5383–5392, 2017.
- [119] R. Jastrzebski, P. Jaatinen, H. Sugimoto, O. Pyrhönen, and A. Chiba, "Design of a bearingless 100 kw electric motor for high-speed applications," in *2015 18th International Conference on Electrical Machines and Systems (ICEMS)*. IEEE, 2015, pp. 2008–2014.
- [120] J. Chen and E. L. Severson, "Optimal design of the bearingless induction motor for industrial applications," in *2019 IEEE Energy Conversion Congress and Exposition (ECCE), September 2019, Baltimore, MD, USA*, May 2019, pp. 1–7.
- [121] Y. Kang and E. L. Severson, "Optimal design of 50kw concentrated winding bearingless motor," in *IEEE Energy Conversion Congress and Exposition (ECCE)*, 2018.
- [122] E. L. Severson, R. Nilssen, T. Undeland, and N. Mohan, "Design of dual purpose no-voltage combined windings for bearingless motors," *IEEE Transactions on Industry Applications*, vol. 53, no. 5, pp. 4368–4379, Sept 2017.
- [123] E. Severson, S. Gandikota, and N. Mohan, "Practical implementation of dual-purpose no-voltage drives for bearingless motors," *IEEE Transactions on Industry Applications*, vol. 52, no. 2, pp. 1509–1518, March 2016.
- [124] K. Ragg, T. Nussbaumer, and J. W. Kolar, "Comparison of separated and combined winding concepts for bearingless centrifugal pumps," *J. Power Electron*, vol. 9, no. 2, pp. 243–258, 2009.
- [125] H. Mitterhofer, B. Mrak, and W. Gruber, "Comparison of high-speed bearingless drive topologies with combined windings," *Industry Applications, IEEE Trans on*, vol. 51, no. 3, pp. 2116–2122, May 2015.
- [126] A. Chiba, K. Sotome, Y. Iiyama, and M. Azizur Rahman, "A novel middle-point-current-injection-type bearingless pm synchronous motor for vibration suppression," *Industry Applications, IEEE Transactions on*, vol. 47, no. 4, pp. 1700–1706, 2011.
- [127] W. Amrhein and S. Silber, "Bearingless single-phase motor with concentrated full pitch windings in interior rotor design," *ISMB8*, 1998.
- [128] J. Huang, B. Li, H. Jiang, and M. Kang, "Analysis and control of multiphase permanent-magnet bearingless motor with a single set of half-coiled winding," *Industrial Electronics, IEEE Transactions on*, vol. 61, no. 7, pp. 3137–3145, July 2014.
- [129] Y. Jiang and E. L. Severson, "Floating capacitor suspension inverter for parallel combined winding bearingless motors," *IEEE Transactions on Industry Applications*, pp. 1–11, 2019.
- [130] Y. Jiang, R. A. Torres, and E. L. Severson, "Current regulation in parallel combined winding bearingless motors," *IEEE Transactions on Industry Applications*, vol. 55, no. 5, pp. 4800–4810, 2019.
- [131] J. Pyrhönen, T. Jokinen, and V. Hrabovcová, *Design of rotating electrical machines*. Wiley. com, 2009.
- [132] T. I. Baumgartner, A. Looser, C. Zwyssig, and J. W. Kolar, "Novel high-speed, lorentz-type, slotless self-bearing motor," in *2010 IEEE Energy Conversion Congress and Exposition*. IEEE, 2010, pp. 3971–3977.
- [133] W. Amrhein, S. Silber, and K. Nenninger, "Levitation forces in bearingless permanent magnet motors," *IEEE Transactions on Magnetics*, vol. 35, no. 5, pp. 4052–4054, 1999.
- [134] T. Schneider and A. Binder, "Design and evaluation of a 60 000 rpm permanent magnet bearingless high speed motor," in *Power Electronics and Drive Systems, 2007. PEDS'07. 7th International Conference on*. IEEE, 2007, pp. 1–8.
- [135] E. Severson, R. Nilssen, T. Undeland, and N. Mohan, "Outer-rotor ac homopolar motors for flywheel energy storage," in *7th IET International Conference on Power Electronics, Machines and Drives (PEMD 2014)*, April 2014, pp. 1–6.



Jiahao Chen (S17M19) received the B.Sc. and Ph.D. degrees in electrical engineering from Zhejiang University, China, in 2014 and 2019, respectively. Since September 2018, he was a visiting scholar at the University of Wisconsin-Madison, USA for one year, where he was involved in bearingless motors. In February 2020, he will be joining Nanyang Technological University, Singapore, as a post-doc researcher. His research interests include electric machines, drives, and direct-drive technologies.



Jingwei Zhu received the B.E. degree in Electrical Engineering and Automation from Zhejiang University, Hangzhou, China, in 2015 and the M.Phil. degree in Electrical Engineering from The Hong Kong Polytechnic University, Hong Kong, in 2018. He was the Edward R. Felber Power Fellowship Scholar at the University of Wisconsin-Madison from 2018 to 2019 where he worked within the Wisconsin Electric Machines and Power Electronics Consortium (WEMPEC). His research interests include the design of novel electric machines, motor drives, and power electronics.



Eric L. Severson (S'09-M'15) received the B.Sc. and PhD degrees in electrical engineering from the University of Minnesota, Minneapolis, USA in 2008 and 2015, respectively where he also worked as a post doctoral associate through 2016. He is currently an assistant professor at the University of Wisconsin-Madison.

Dr. Severson is an associate director of the Wisconsin Electric Machines and Power Electronics Consortium (WEMPEC) and fellow of the Grainger Institute for Engineering. His research interests include design and control of electric machines and power electronics, with focus areas in magnetic bearings, bearingless motors, flywheel energy storage, and off-highway vehicle electrification.

Dr. Severson is the 2019 Vice Chair of the IEEE IAS/PES Joint Chapter in Madison, WI, USA. He is a recipient of the USA National Science Foundation CAREER Award in 2020, the Department of Defense NDSEG fellowship in 2009, and the National Science Foundation Graduate Research Fellowship in 2009.